Received: 12 June 2024 | Revised: 9 December 2024 | Accepted: 12 December 2024

DOI: 10.1111/joa.14207

Journal of Anatomy | ANATOMICAL SOCIETY | WILEY

ORIGINAL ARTICLE

Achilles tenocytes from diabetic and non diabetic donors exposed to hyperglycemia respond differentially to inflammatory stimuli and stretch

Nils Fleischmann[1] | Sarah Hofmann[1] | Clemens Gögele[1] | Eva Frank[1] | Christian Werner[1] | Maria Kokozidou[1] | Bernd Hoffmann[2] | Jens Konrad[2] | Gundula Schulze-Tanzil[1]

[1]Institute of Anatomy and Cell Biology, Paracelsus Medical University, Nuremberg, Germany

[2]Institute of Biological Information Processing, IBI-2: Mechanobiology, Research Centre Juelich, Juelich, Germany

Correspondence
Gundula Schulze-Tanzil, Institute of Anatomy and Cell Biology, Paracelsus Medical University, Prof.-Ernst-Nathan Str. 1, 90419 Nuremberg and Salzburg, Nuremberg, Germany.
Email: gundula.schulze@pmu.ac.at

Funding information
Kerscher'sche Diabetes Research Foundation, Grant/Award Number: SZ_FP_008.18 and SZ_FP_164.20; Deutsche Forschungsgemeinschaft, Grant/Award Number: SCHU1979/14-1

Abstract

Diabetes mellitus type 2 (DMT2) promotes Achilles tendon (AS) degeneration and exercise could modulate features of DMT2. Hence, this study investigated whether tenocytes of non DMT2 and DMT2 rats respond differently to normo- (NG) and hyperglycemic (HG) conditions in the presence of tumor necrosis factor (TNF)α or cyclic stretch. AS tenocytes, isolated from DMT2 (fa/fa) or non DMT2 (lean, fa/+) adult Zucker Diabetic Fatty (ZDF) rats, were treated with 10 ng/mL TNFα either under NG or HG conditions (1 g/L vs. 4.5 g/L glucose) and were exposed to cyclic stretch (14%, 0.3 Hz, 48 h). Tenocyte survival, metabolic activity, gene and/or protein expression of tendon extracellular matrix component *collagen type 1*, *alpha smooth muscle actin* (*αSMA*, *Acta2*), the stress defense enzyme *heme oxygenase-1* (*Hmox1*) as well as *suppressors of cytokine signaling* (*Socs*)*1* and *Socs3* were analyzed. Tenocyte vitality remained high, but metabolic activity was slightly impaired by HG conditions irrespectively of cell origin. *Collagen type 1 alpha* protein and gene expression was suppressed by TNFα, but only in cells of non DMT2 animals in NG culture medium. Higher amounts of αSMA were visualized in tendons/tenocytes of diabetic rats or those exposed to TNFα. Cyclic stretch caused cell alignment in zero stretch direction. In addition, it led to a significant reduction of cell perimeters, particularly in cells of DMT2 donor rats under HG conditions. *Hmox1*, *Socs1* and *Socs3* were induced by HG, but only in tenocytes of diabetic rats (4 h). Stretch induced significantly *Hmox1* transcriptional activity under NG conditions and *Socs3* under HG conditions especially in tenocytes of DMT2 rats. The response of tenocytes to TNFα and cyclic stretch depends on glucose supply and origin suggesting their irreversible impairment by DMT2.

KEYWORDS
Achilles tendon, cyclic stretch, cytokine, diabetes mellitus type 2, tendinopathy, tenocytes, TNFα

Nils Fleischmann and Sarah Hofmann shared first authorship.

1 | INTRODUCTION

Tendon degenerations, so called tendinopathies, restrict patients working capability and life quality due to chronic pain and impaired tendon function. Particularly Achilles (AS) and patellar tendons are prone to tendinopathy (Aicale et al., 2020). Despite the fact that pathogenesis is still poorly understood, the molecular background for unsuccessful AS healing as precondition for tendon degeneration has been discussed previously (Schulze-Tanzil et al., 2022). AS tendinopathy represents a common reason for chronic pain and restricted movements in the ankle joint. It could result from relative overload and repeated microinjuries of the AS. The AS is the largest and strongest tendon of the body (Ballal et al., 2014) and hence, prone to injury (Hess, 2010; Tarantino et al., 2023). Diabetes mellitus (DM) type 2 (DMT2) is a well known predisposition for tendon injury, impaired healing (Chbinou & Frenette, 2004; Egemen et al., 2012) and subsequent tendinopathy (Cannata et al., 2021; Lui, 2017). Patients with DMT2 showed more often AS degenerations than age and sex matched healthy individuals (Afolabi et al., 2021). DMT2 associated AS degeneration can lead to its rupture (Tarantino et al., 2023). Structural changes such as disorganized fibers and calcification could be shown in diabetic AS tendons (Batista et al., 2008; Partridge & Rajbhandari, 2017). Biomechanical properties change in DM rat Achilles tendon (rAS) (de Oliveira et al., 2011, 2012) and those of humans (Guney et al., 2015). The development of altered biomechanics of the AS (e.g., changes of the E-modulus) associated with tendinopathic degeneration related to DMT2 could also be enhanced by other DMT2 associated musculoskeletal impairments, such as the diabetic foot (Batista et al., 2008). Even the feeding of rats with a high glucose diet induced changes in healing tendon tissue (Korntner et al., 2017). The oversupply of glucose facilitates glycation of cell and extracellular matrix (ECM) components. Accumulation of advanced glycation end products (AGEs) is well known in DMT2 (Patel et al., 2019) and AGEs cause metabolic changes as shown in vitro (Patel et al., 2019). AGE formation could also explain some biomechanical alterations in tendons due to their effects on ECM components (Lee & Veres, 2019) e.g., by reducing collagen fiber sliding (Li et al., 2013). Tenogenic differentiation capacity of rat tendon derived stem cells was impaired under HG and DM conditions. Compared to tenogenic lineage differentiation the chondrogenic/osteogenic commitment was superior (Kim et al., 2021; Shi et al., 2019), which was influenced by AGEs (Shi et al., 2021). Stem cells are important for tendon healing (Vaidya et al., 2023) and healing is diminished in DMT2 (Vaidya et al., 2023). The transition of fibroblasts in a myofibroblastic phenotype is important in normal wound closure and healing (Cherng et al., 2008). Therefore, this transition plays a role in diverse healing processes, fibrotic disease (Cherng et al., 2008) and hypertrophic scarring (Wang et al., 2008), but also in degenerative tissue changes e.g., of the liver in diabetic rats (Attia et al., 2021). Alpha Smooth muscle actin (αSMA) is a crucial marker of myofibroblasts (Cherng et al., 2008). Tenocytes in isolated lax fascicles of tendons are able to contract by enhancing their αSMA expression (Gardner et al., 2012). Tenocytes can exert mechanical forces on the extracellular tendon matrix (ECM) reflected by αSMA expression, but are also in need of a mechanical stretch challenge for survival and healing (Egerbacher et al., 2008).

Adapted exercise is known to stimulate tendon healing (Eliasson et al., 2012a, 2012b). It inhibits the progression of AS tendinopathic changes by DMT2 (Bezerra et al., 2016), improves biomechanical properties of tendons in a diabetic rat model (de Oliveira et al., 2012) and could counteract insulin resistance as the main feature of DMT2 (Zhang et al., 2023). Heme oxygenase (HMOX)1 is an enzyme involved in tissues' protection from injury, which was suppressed by pro-inflammatory cytokines such as IL-1β and TNFα and upregulated by IL-10 in chondrocytes (Fernandez et al., 2003; Guillen et al., 2008; Tognoloni et al., 2023). This regulation might be cell-type specific since Clikeman et al., reported an induction of HMOX1 by TNFα in endothelial cells (Terry et al., 1999). HMOX1, an antioxidative enzyme involved in cellular stress has been implicated as a putative target in DMT2 in a study in a rat DM model (El-Huneidi et al., 2021; Immenschuh & Ramadori, 2000). High extracellular glucose levels alter cellular response to oxidative stress (Poulsen et al., 2014). Platelet extract upregulated HMOX1 by the Nuclear Factor Erythroid-derived 2-like 2 (Nrf2)/extracellular signal regulated kinase (ERK) pathway. The same Nrf2/ERK signaling cascade protected rats from diabetic retinopathy (Huo et al., 2022). However, it is unclear whether the *Hmox1* gene activity is also regulated by exercise. In addition to HMOX1 suppressors of cytokine signaling (SOCS)1 and 3 could exert protective functions by downregulating proinflammatory cytokine signaling. Both are negative feedback regulators of proinflammatory cytokine signaling (John et al., 2010). In a previous study with human Hamstring tenocyte cultures derived from healthy tendons a 24 h stimulation with TNFα induced SOCS1 and SOCS3. Although data concerning the mechanoregulation of the *Socs1* and *Socs3* genes in tendon are not available, proinflammatory cytokines are amplified by stressful exercise such as IL-6 (Skutek et al., 2001). In concert with *Hmox1* gene activity, those of *Socs1* and *3* could present an important strategy to limit inflammation under HG conditions. Both SOCS proteins are associated with the JAK/STAT signaling cascade (de Souza et al., 2011). A recent study comparing the gene expression pattern in rotator cuff tendon samples of non DMT2 and DMT2 donors, identified by single cell RNA-seq that genes of the JAK/STAT signaling pathway were differentially expressed in both patient populations (Yuan et al., 2024).

Based on these considerations, a HG versus NG model was used in the present study as an in vitro approach to investigate whether tenocytes from healthy or diabetic tendons respond in a different manner to a proinflammatory challenge or exercise. TNFα was used as proinflammatory mediator to induce tenocyte stress according to a previous study (John et al., 2010). For characterizing the mechanoresponse of tenocytes isolated from non DMT2

and DMT2 donors, a well-standardized training model was applied (Gögele et al., 2021).

2 | METHODS

2.1 | Sample and cell origin

Adult male non DMT2 heterozygous (fa/+, $n=7$) Zucker Diabetic Fatty (ZDF) and diabetic homozygous (fa/fa, DMT2, $n=7$) rats derived from Charles River Laboratories International, Inc., (Sulzfeld, Germany). Rats received a specific diabetogen high protein diet (Purina 5008, Firma sSniff, Spezialdiäten GmbH). The presence of hyperglycemia associated with DMT2 was demonstrated by blood glucose measurements (spot tests, AlphaTrak 2, Zoetis, Tullytown, PA, USA). Two or three rats per cage were housed in standardized living conditions in a special incubator (55% humidity, 21 ± 2°C, Memmert GmbH and co.KG, Schwabach, Germany).

Rats were finalized at the age of 6–7 month as part of another project (animal approval: RUF 55.2.2-2532-2-729-17). Rat AS (rAS) were explanted post mortem for the current project.

2.2 | Histology

, Tendons were fixed 24 h in 4% paraformaldehyde (PFA/in phosphate buffered saline [PBS], Santa Cruz Biotechnology Inc., Dallas, Texas, USA) and embedded in paraffin using a pathcenter (Shandon Pathcenter, Thermo Scientific, Waltham, Massachusetts, USA). Paraffin sections (7 µm thick) were prepared and melted on glass slides in an oven (Memmert GmbH and co.KG) at 60°C overnight before deparaffinized 2 × 5 min in xylene (Carl Roth GmbH and Ko.KG, Karlsruhe, Germany) and rehydrated in a descending ethanol solution series (ETOH, 99.8%, 96%, 80%, 70%, Carl Roth GmbH and Ko.KG). Sections were stained with hematoxylin eosin (HE), alcian blue (AB) and picrosirius red (SR).

2.2.1 | HE stain

For HE stain, sections were incubated 6 min in Harry's hematoxylin (Carl Roth GmbH and Ko.KG), rinsed in running tap water and then, counterstained with eosin for 4 min (Carl Roth GmbH and Ko.KG).

2.2.2 | AB stain

AB stain (pH 2.5) was undertaken to visualize deposition of sulphated glycosaminoglycans by a blue color. Deparaffinized sections were incubated for 3 min in 1% acetic acid (Carl Roth GmbH and Ko.KG) and then, for 30 min in 1% AB in acetic acid (Carl Roth GmbH and Ko.KG) before rinsed in 3% acetic acid. Nuclear fast red aluminum sulphate solution (Carl Roth GmbH and Ko.KG) was used for counterstaining cell nuclei for 5 min.

2.2.3 | SR stain

SR staining depicts the distribution of collagen type 1 and 3 (Lattouf et al., 2014). Deparaffinized sections were rinsed in nondistilled (nondist.) water for 4 min. Eight minutes staining in Weigerts hematoxylin (MORPHISTO GmbH, Frankfurt am Main, Germany) allowed visualization of cell nuclei. Then, sections were washed with distilled (dist.) water for 5 s, rinsed in nondist. water for 10 min and in dist. water again for 1 min. Sections were immersed in SR (MORPHISTO GmbH) staining solution for 60 min, before two-times (1 min) incubated in 30% acetic acid (Carl Roth GmbH and Ko.KG) and then, two-times in 96% ETOH for 4 min.

2.2.4 | Sample mounting and observation

After all staining procedures sections were dehydrated in an ascending alcohol series (70%, 80%, 96% and 99.6% ETOH) before covered with Entellan (Merck KGaA). Histological staining was photodocumented using a light microscope (DM1000 LED, Leica Microsystems GmbH, Wetzlar, Germany) and Flexacam C3 camera (Leica Microsystems). HE and AB stain of the rAS of the controls (fa/+) and diabetic rats were histopathologically analyzed using the Movin tendinopathy scoring system (Maffulli et al., 2008).

2.3 | Tenocyte isolation from rAS

Tenocytes were isolated from the left rAS using explant culture. Loose connective tissue, fascia and peritenon were discarded and small tissue segments (2 mm) of pure tendon were placed in T25 flasks (CellPlus, Sarstedt AG, Nümbrecht, Germany) with growth medium 96% [v/v] DMEM/Ham's F-12 [1:1] supplemented with stable L-glutamin, 1% [v/v] amphotericin B, 1% [v/v] MEM amino acids, 1% [v/v] penicillin/streptomycin, 1% [v/v] ascorbic acid supplemented (all products from Carl Roth GmbH) and 10% fetal bovine serum (FBS, Pan-Biotech GmbH, Aidenbach, Germany). Tenocytes emigrated in the next 7–10 days from the tissue on the growth surface of the flasks. First passage tenocytes were cryoconserved to be stored in liquid nitrogen and then, thawed, recultured and expanded for the experiments (passages 4–6).

2.4 | Tenocyte culture

Cryoconserved tenocytes derived from rAS were gently thawed at room temperature, seeded into T75 flasks with 10 mL of the above mentioned growth medium (37°C, 5% CO_2) and expanded by subsequent passaging. For the experiments tenocytes were seeded at

10,000 cells/cm^2 in T25 flasks and let adhere for 24 h before exposed to hyper- (HG, 4.5 g/L) and normoglycemic (NG, 1 g/L) conditions with or without the proinflammatory cytokine TNFα (10 ng/mL, Peprotech, Hamburg, Germany).

2.5 | Alamarblue assay with rAS tenocytes

31,250 cells/cm^2 were seeded into 96-well plates (Sarstedt) with 100 µL growth medium as triplicates. After 24 h of cell adherence and after 18 h of stimulation, 25 µL of CellTiterBlue solution (ThermoFisher Scientific Inc., Waltham, USA) was added to the wells. The colour change due to metabolic activity was assessed hourly (at wavelengths 600 and 570 nm) using a plate reader (Tecan Austria GmbH, Grödig, Austria) and the final results of 6 h were calculated.

2.6 | Cell vitality assay

Tenocytes were cultured and stimulated on cover slips. For visualization of live and dead cells cover slips were incubated with 50 µL fluoreceindiacetate (FDA)/propidiumiodide (PI) solution for 3 min and photographed using confocal laser scanning microscopy (CLSM, SPEII, Leica Microsystems).

The staining solution was prepared by combining 5 µL/mL FDA (Sigma-Aldrich, Munich, Germany, 3 mg/mL stock solution in acetone) with 1 µL/mL PI (1% solution, Carl Roth GmbH and Ko.KG) in PBS.

2.7 | Immunohistology and -cytochemistry

Immunofluorescence labeling was performed to localize and compare the expression of αSMA and collagen type 1 in the rAS in situ and in in vitro cultured rAS tenocytes of the DMT2 and control animals. Cell nuclei were counterstained using 4′,6′-diamidino-2-phenylindole (10 µg/mL, DAPI, Roche, Mannheim, Germany).

Deparaffinized sections or tenocytes cultured at 1000 cells/cm^2 on Poly-L lysine coated cover slips placed in 12 well plates or at 12,500 cells/cm^2 on silicone stretching chambers were fixed in 4% PFA for 15 min, before gently rinsed three times in TRIS buffered saline (TBS: 0.05 M TRIS, 0.015 M NaCl, pH 7.6). A blocking step with protease-free blocking solution (5% donkey serum diluted in TBS with 0.1% Triton X 100 for cell permeabilization) for 20 min at RT followed. Tissue sections or tenocytes were incubated with the primary antibodies overnight diluted in blocking solution, at 4°C, in a humidifier chamber (Table 1). When controls were stained, the primary antibodies were omitted. Samples were rinsed three times with TBS and then incubated with the secondary antibodies (cyanine[cy]3—donkey-anti-mouse or Alexa-Fluor488-coupled-anti-goat), diluted 1:200 in TBS, for 1 h at RT. To depict the actin-cytoskeleton, tenocytes were stained with phalloidin-Alexa-Fluor488 in blocking buffer. Rinsing in TBS (three times for 5 min) followed, before sections were covered with Fluoromount G (Biozol Diagnostica Vertrieb GmbH, Eching, Germany). Photos were taken with the CLSM. Photos of three different microscopic fields were analyzed for the calculations of relative fluorescence intensities using the software "ImageJ program". The used version was (1.53n/7 November 2021: ImageJ bundled with 64-bit Java 1.8.0_172 [70 MB]).

2.8 | Preparation of PDMS chambers

Elastomeric chambers were casted using Sylgard 184 silicone (Ellsworth, WI, USA) with a crosslinker ratio of 40:1 as described previously (Gögele et al., 2021). Silicone was filled into a 50 mL syringe and degassed, before 5 mL was released without any air bubbles into the polysterol casting frames. Thermic crosslinking followed at 60°C for 16 h. Polymerized silicone chambers (Young's modulus of 50 kPa), remained at RT and were protected from ultraviolet light until use. Chambers fixed already in the stretching frame were disinfected with isopropanol (Carl Roth GmbH and Ko.KG) and left to dry overnight under sterile conditions. The chambers had a square bottom cell culture area of 4 cm^2. The thickness of the stretched bottom of the chamber was 0.5 mm, the outer rim around the seeded area: 0.5 cm wide and 4 mm high.

2.9 | Stretch assay

Tenocytes were cultured on silicone chambers at 12,500 cells/cm^2 and let to adhere for 48 h before exposed to uniaxial cyclic stretch (14% at 0.3 Hz, 48 h for further details, see Gögele et al., 2021) under NG and HG conditions within the incubator using a stretching device (6× cell stretcher) activated by a linear stepper motor (MT63, Steinmeyer Mechatronik GmbH, Dresden, Germany) and LabVIEW

TABLE 1 Antibodies and staining used.

Target	Primary antibody	Dilution	Secondary antibody	Dilution
Collagen type 1 A1	Goat-anti-human (COL1A1 chain), Abcam, (Ab58595), Cambridge, UK	1:50	Donkey-anti-goat; Alexa-Fluor488-coupled, Invitrogen, Carlsbad, California, USA	1:200
Phalloidin-Alexa-Fluor488	Santa Cruz Biotechnologies, Santa Cruz, (Sc-363791), California, USA	1:100	None	None
α-Smooth muscle (SMA) actin	Mouse-anti-human, Sigma-Aldrich, (A5228), Munich, Germany	1:50	Donkey-anti-mouse; Cyanine-3 coupled, Invitrogen, Carlsbad, California, USA	1:200

software (version 2.0) as described previously (Gögele et al., 2021). Before starting cyclic stretching, the mechanical stretcher was calibrated at the zero-position with the help of the appropriate calibration plate of the device.

2.10 | RNA isolation and reverse transcription and qRT-PCR

Tenocytes in T25 flasks or silicone chambers were lysed for 5 min in RLT buffer (Qiagen GmbH, Hilden, Germany) with 0.1% mercaptoethanol. RNA was isolated and purified using the RNeasy Mini kit according to the manufacturer's recommendation (Qiagen GmbH) with an on-column DNA isolation through action of DNAse. Purity of the isolated RNA was controlled at the 260/280 absorbance ratio for RNA purity and RNA concentration measured using the Nanodrop ND-1000 spectrophotometer (Peqlab, Biotechnologie GmbH, Erlangen, Germany).

Isolated total RNA (125 ng) was reversely transcribed into cDNA using the QuantiTect Reverse Transcription Kit (Qiagen), according to the manufacturer's protocol with the TaqMan Gene Expression Assay (Life Technologies). Rat specific primer pairs (Table 2) were used with Hypoxanthine-guanine-phosphoribosyltransferase (*Hprt1*) as a reference gene and collagen type 1 alpha 1 chain (*Col1a1*), smooth muscle actin (Acta2), heme oxygenase (*Hmox*)1, suppressors of cytokine signaling 1 and 3, (*Socs1*, *3*) as genes of interest. qRT-PCR was performed using the real-time PCR detector StepOnePlus (Applied Biosystems [ABI], Foster City, CA, USA) thermocycler with StepOnePlus software 2.3 (ABI). The mean normalized expressions of the genes of interest were assessed related to the reference gene (*Hprt1*) and calculated for each sample relying on the method introduced by Schefe et al., (Schefe et al., 2006).

2.11 | Statistical analyses

Statistics were performed with GraphPad Prism8 (GraphPad software Inc., San Diego, USA). For comparison between groups, a two-tailed one-way ANOVA (Fisher), for comparison with the control group, depending on experimental setting the unpaired or paired *t*-test was used followed by Tukey's multiple comparison post hoc testing. The level of significance/confidence interval was set at p values of ≤0.05 (*), ≤0.01 (**), ≤0.005 (***) and $p \leq 0.001$ (****).

3 | RESULTS

3.1 | Cell donor characteristics

The body weight of both rat groups differed slightly at the time point of finalization (mean: fa/+: 391.71 ± 24.47, fa/fa: 398.71 ± 34.74, not significant, age: 211–223 days, Figure 1a). However, the differences between the body weights of non DMT2 and DMT2 were highly significant 3 month before finalization (age: 99–107 days) and at the age, when the rats were introduced into the facility (age: 71–75 days) (Figure 1a). DMT2 rats (fa/fa) used as tenocyte donors or for in situ analysis of tendons showed continuously and significantly elevated blood glucose levels (mean: fa/fa: 32.2 ± 5.82 mmol/L, at finalization) compared to heterozygous animals (mean: fa/+: 9.04 ± 1.19 mmol/L, at finalization). These significant differences between both cohorts were already detectable at the age of 71–75 days and did not differ comparing the various time points of measurement (Figure 1b). In addition, typical clinical and histopathological features of DMT2 such as polydypsia, polyuria, sporadic gingival infection, cataract, pancreas degeneration and nephropathies were observed (not shown).

3.2 | In situ histopathological evaluation of rAS of non DMT2 and DMT2 rats

For the histopathological analyses the rAS midsubstance was dissected (Figure 1c). The HE stain revealed differences in density of collagen fiber bundles and fiber arrangement (Figure 1c1,d1). The GAG content was slightly higher in many of the rAS of DMT2 donors as visualized by the AB stain (Figure 1c2,d2). SR revealed light microscopically the densely organized collagen of the rAS of both donor groups in orange-red. The polarized light allowed to distinguish fiber orientation and density of collagen type 1 and 3 fiber bundles (Figure 1c3,c4,d3,d4). Tendons explanted from

TABLE 2 Rat-specific primers used for qRT-PCR.

Gene symbol	Gene name	Assay ID	Amplicon length (bp)	Efficacy	NCBI gene reference
Col1a1	*Collagen type 1, alpha 1*	Rn01463848_m1	115	2.01	NM_053304.1
Hmox1	*Heme oxygenase-1*	Rn00561387_m1	132	1.96	NM_012580.2
Hprt1	*Hypoxanthine-guanine-phosphoribosyltransferase*	Rn01527840_m1	64	1.98	NM_012583.2
Acta2	α-Smooth muscle actin	Rn01759928_g1	65	1.96	NM_031004.2
Socs1	*Suppressor of cytokine signaling 1*	Rn00595838_s1	76	2.09	NM_145879.2
Socs3	*Suppressor of cytokine signaling 3*	Rn00585674_s1	73	1.9	NM_053565.1

Note: All primers were obtained from ThermoFisher Scientific (Germany).
Abbreviation: bp, base pairs.

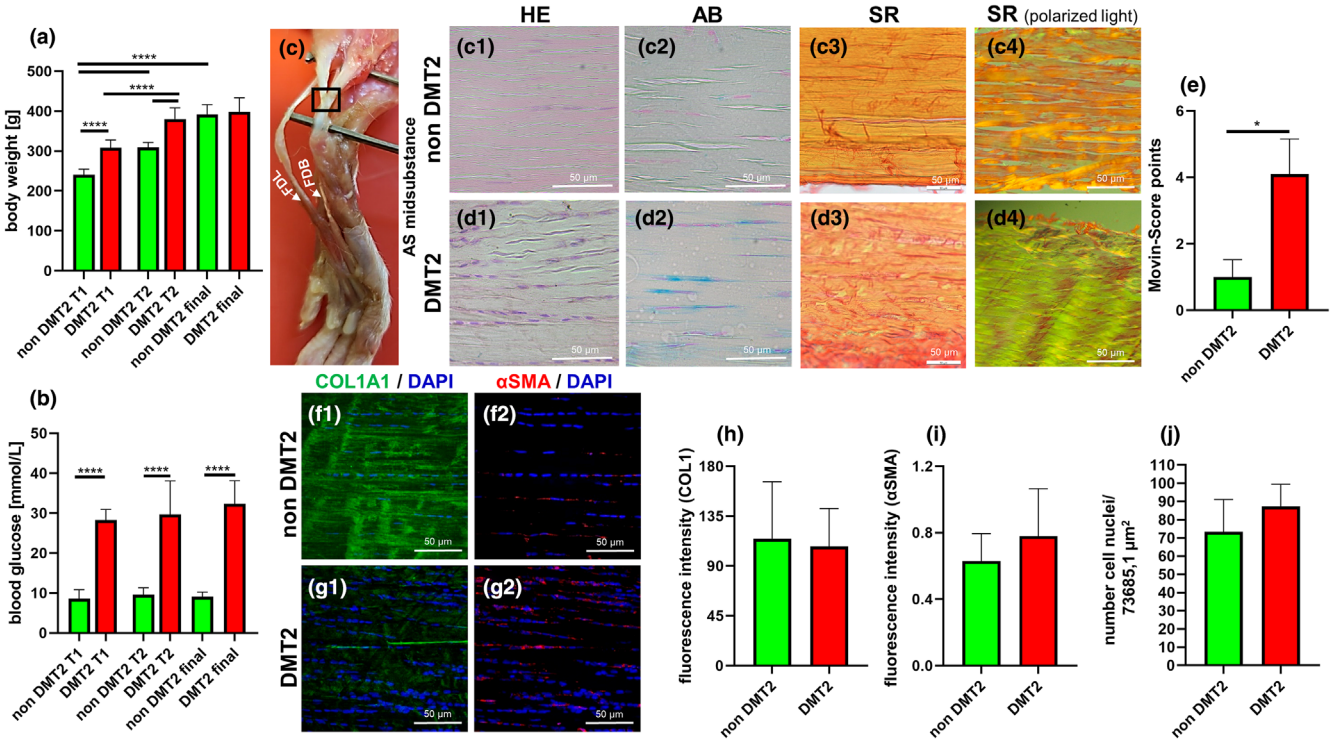

FIGURE 1 Histology and immunohistology of Achilles tendons of non diabetic (non DMT2) and diabetic rats (DMT2). Body weights (a) and blood glucose levels (b) of non DMT2 and DMT2 cell donor rats at the age of 71–75 days (T1), 99–107 days (T2) and immediately before finalization at the age of 211–223 days (final). (c) Gross anatomical image of the Achilles (AS) tendon of a ZDF rat. FDB, Flexor digitorum brevis tendon; FDL, Flexor digitorum longus tendon. (c1, d1) Hematoxylin–eosin (HE), (c2, d2) Alcian blue (AB), (c3–c4, d3–d4) Picrosirius red (SR) stain, (c3, d3) Non polarized light, (c4, d4) Polarized light. (e) Tendon degeneration was evaluated using Movin Score. (f1, g1) Collagen type 1 α1 chain (COL1A1, green) and (f2, g2) alpha smooth muscle actin (αSMA, red) immunofluorescence labeling. Cell nuclei are counterstained using 4′,6′-diamidino-2-phenylindole (DAPI, blue). Relative fluorescence intensity of COL1A1 (h) and alpha smooth muscle actin (i) is calculated. (j) Number of cell nuclei per microscopic field. DMT2, diabetes mellitus type 2. Scale bars: 50 µm. $n = 5–7$ tendons from non DMT2 or DMT2 rats. Unpaired *t*-test, **p*: 0.05, *****p*: 0.0001.

diabetic and non DMT2 animals were histopathologically analyzed using the Movin score (Maffulli et al., 2008). Significantly higher Movin score values associated with a higher sum of observed degenerative criteria were detected in rAS of rats suffering from DMT2 (Figure 1e) compared to controls. Typical degenerative features observed were more inhomogenous cell distribution, more rounded cell nuclei, lesser density and alignment of collagen fibers as well as slightly elevated sGAG deposition.

3.3 | In situ immunohistological evaluation of rAS of non DMT2 and DMT2 rats

There was a trend of slightly more collagen type 1 detectable in rAS from non DMT2 animals compared to those explanted from DMT2 rats (Figure 1f1,g1,h, not significant). Since αSMA is involved in wound healing, but also scar formation (Kim et al., 2008; Wang et al., 2008) it was investigated in this study. αSMA protein was higher expressed in rAS of DMT2 animals compared to those without DMT2 (Figure 1f2,g2,i, not significant). rAS from DMT2 animals showed more cell nuclei (Figure 1j, not significant) and hence, higher cellularity.

3.4 | Vitality and metabolic activity of rAS tenocytes of non DMT2 and DMT2 rats under NG or HG conditions

Tenocyte vitality remained high (mean: 98.87 ± 1.1%) and was not significantly affected by the treatment regimes neither by NG versus HG (with/without 10 ng/mL TNFα) nor by the cell donor (non DMT2 vs. DMT2 rats) (Figure 2a–c).

The metabolic activity was slightly impaired under HG conditions compared to the NG control in both tenocyte donor groups. It was also impaired by TNFα in tenocytes of non DMT2 and DMT2 donors, but only under NG and not under HG conditions (not significant) (Figure 2d).

3.5 | Nuclear area of rAS tenocytes of non DMT2 and DMT2 rats under NG or HG conditions

TNFα led to a decrease of the nuclear size (area) in tenocytes deriving from non DMT2 and DMT2 rats. A lower nuclear size was generally observed in tenocytes isolated from the non DMT2 rats, when stimulated with TNFα and/or HG (24 h, Figure 2e, not significant).

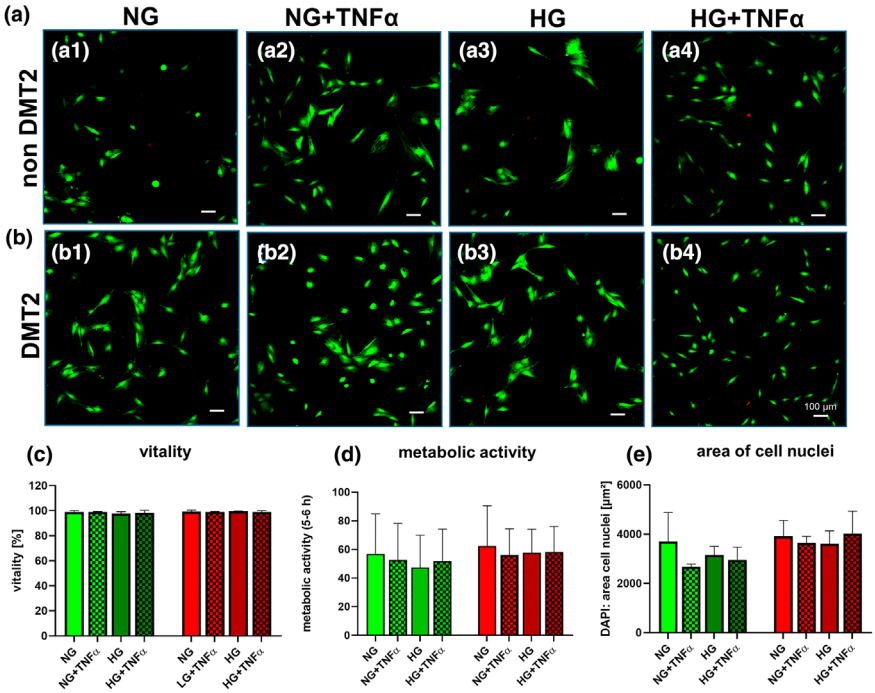

FIGURE 2 Vitality, metabolic activity and area of cell nuclei of tenocytes derived from non diabetic (non DMT2) and diabetic (DMT2) rats exposed to NG vs. HG conditions with or without TNFα. (a, b) Live-death assay (24 h) performed with tenocytes of non DMT2 (a) and DMT2 (b) rats. Vital cells are green and dead cells red. (c) Percentage of living cells. (d) Metabolic activity of tenocytes after 6 h of culture. (e) Area of cell nuclei (24 h) based on 4′,6′-diamidino-2-phenylindole stain. $n = 3$ independent experiments with tenocytes of either DMT2 or non DMT2 rats were conducted. Tenocytes were treated with 10 ng/mL tumor necrosis factor α (TNFα), either under normoglycemic (NG) or hyperglycemic (HG) conditions. Scale bars: 100 µm.

3.6 | ECM, cytoskeletal and cell surface ECM protein expression of rAS tenocytes from non DMT2 and DMT2 rats

Collagen type 1 protein expression was suppressed by TNFα under NG condition but only in tenocytes of non DMT2 animals after 24 h (Figure 3a,b, not significant). The same trend was evident at the gene expression level (Figure 3c). Collagen type 1 protein expression was generally higher in tenocytes of DMT2 animals (Figure 3a,b).

Higher amounts of αSMA protein were visualized in tenocytes exposed to TNFα, irrespectively of their donor origin (fa/+ = non DMT2 vs. fa/fa = DMT2) and glucose content of culture medium (HG, NG) (Figure 3d, not significant). αSMA was generally higher expressed in tenocytes of diabetic animals (Figure 3e, not significant). The inductive effect by TNFα was reflected on the gene expression level.

3.7 | Gene expression analyses of rAS tenocytes derived from non DMT2 or DMT2 animals under NG or HG conditions

In tenocytes from DMT2 donors, *Hmox1* was more than twofold induced by HG at 4 h but not at 24 h. At 24 h, it was more than threefold induced by TNFα under both conditions (NG and HG), but only in tenocytes of non DMT2 rats (Figure 4a1,a2). *Socs1* was also more than twofold induced by HG at 4 h, but only in tenocytes of DMT2 rats (Figure 4b). At 24 h *Socs1* was suppressed by HG, but only in tenocytes of non DMT2 rats. *Socs3* gene transcription revealed no major changes (more than twofold) in tenocytes of non DMT2 and DMT2 rats (Figure 4c). Comparing the expression levels of these genes in tenocytes of non DMT2 and DMT2 rats there was no significant difference, but a trend of lower *Hmox1* expression in cells of DMT2 rats at the 4 h investigation time point (Figure S1).

3.8 | rAS tenocyte response to cyclic stretch under NG and HG conditions

Tenocytes of non DMT2 and DMT2 rats were exposed to cyclic stretch either under NG or HG conditions. Tenocytes, irrespectively of origin (non DMT2 or DMT2) and culture conditions (NG or HG), survived 24 and 48 h cyclic stretching on silicone surfaces (Figure 5a1–a8). They showed a typical cell alignment after 48 h of stretch in direction of zero stretch with no visible differences between NG and HG conditions and cell origin (Figure 5a2,a6,a4,a8). Most of the tenocytes showed prominent F-actin stress fibers (Figure 5b1–b8). The majority of them was aligned according to zero stretch direction in the stretched tenocytes. Cells exhibited some immunoreactivity for αSMA, particularly, at focal adhesion sites with no major difference between unstretched and stretched cells (Figure 5b1–b8).

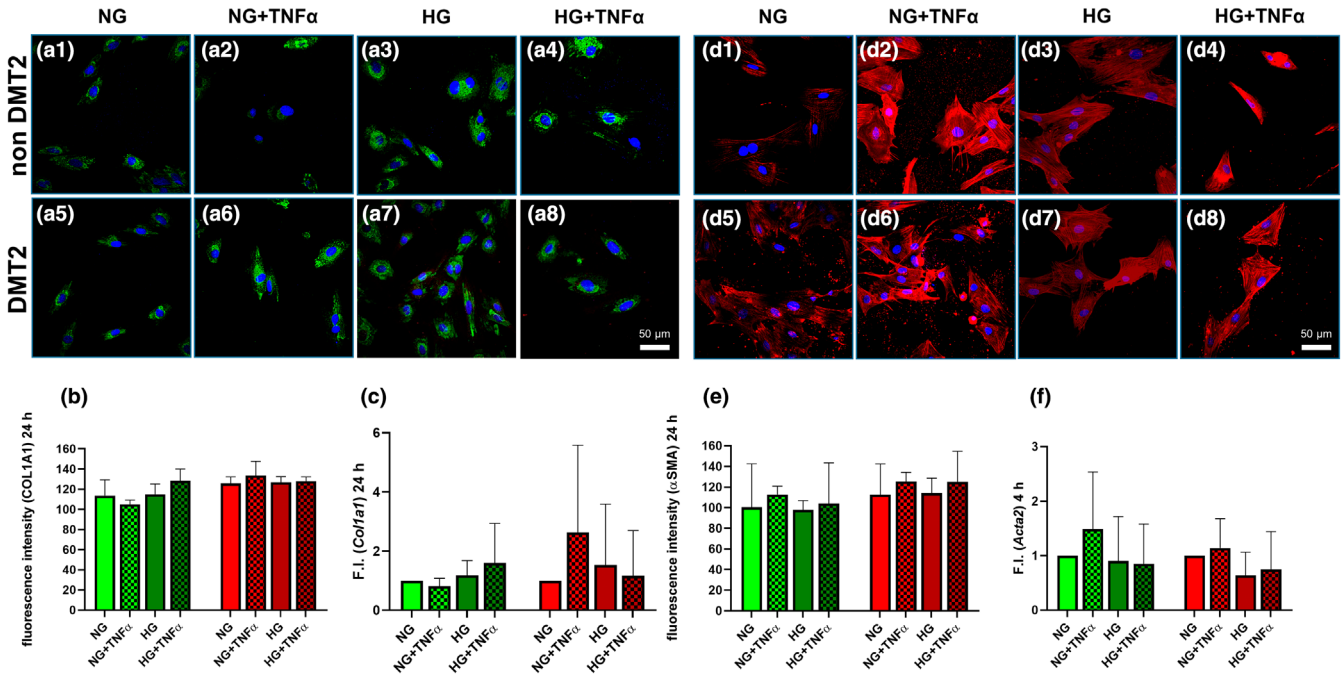

FIGURE 3 Collagen type 1 alpha 1 chain (COL1A1) and alpha smooth muscle actin (αSMA) expression profile of cultured tenocytes of non diabetic (non DMT2) and diabetic (DMT2) rats exposed to normoglycemic (NG) and hyperglycemic (HG) conditions with or without TNFα. Protein expression was visualized by immunocytochemistry. Representative images of collagen type 1 (a1–a8: COL1A1: Green) and alpha smooth muscle actin (d1–d8: αSMA: Red) expression are depicted. Cell nuclei were counterstained using 4′,6′-diamidino-2-phenylindole (DAPI, cell nuclei: Blue). (b) Densitometric evaluation of COL1A1 protein expression (24 h) shows relative fluorescence intensity. (c) Gene expression of *collagen type 1 alpha1* chain (*Col1a1*, 24 h) is depicted. (a1–a4, d1–d4) Tenocytes of non DMT2, (a5–a8, d5–d8) tenocytes of DMT2 are shown. (e) Analysis of αSMA fluorescence intensity. (f) Alpha smooth muscle actin (*Acta2*) gene expression (4 h) is depicted. *Hypoxanthine-guanine-phosphoribosyltransferase (Hprt)1* was used as a reference gene for gene expression analyses (c, f). F.I., fold increase. Gene expression data are normalized to the NG controls (c, f). Tenocytes were treated with 10 ng/mL tumor necrosis factor α (TNFα), either under normoglycemic (NG) or hyperglycemic (HG) conditions. Scale bars: 50 µm. $n = 3$ independent experiments with tenocytes of either non DMT2 or DMT2 rats were conducted.

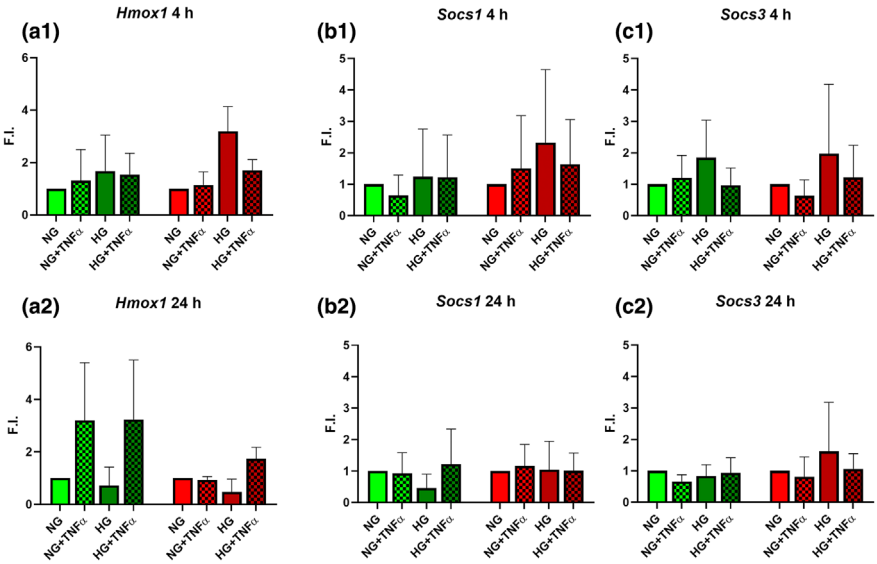

FIGURE 4 Gene expression of tenocytes isolated from non diabetic (non DMT2) and diabetic (DMT2) rats exposed to NG vs. HG conditions with or without TNFα. (a1, a2) *Heme oxygenase* (*Hmox1*, 4 h, 24 h), (b1, b2) *suppressor of cytokine signaling (Socs)1*, 4 h, 24 h, (c1, c2) suppressor of cytokine signaling (Socs)3, 4 h, 24 h. Hypoxanthine-guanine-phosphoribosyltransferase (Hprt)1 was used as a reference gene. F.I., fold increase. Data of NG was normalized to 1 in tenocytes of non DMT2 and DMT2 rats. $n = 3$ independent experiments with tenocytes of either $n = 3$ non DMT2 or $n = 3$ DMT2 rats were conducted. Tenocytes were treated with 10 ng/mL tumor necrosis factor α (TNFα), either under normoglycemic (NG) or hyperglycemic (HG) conditions.

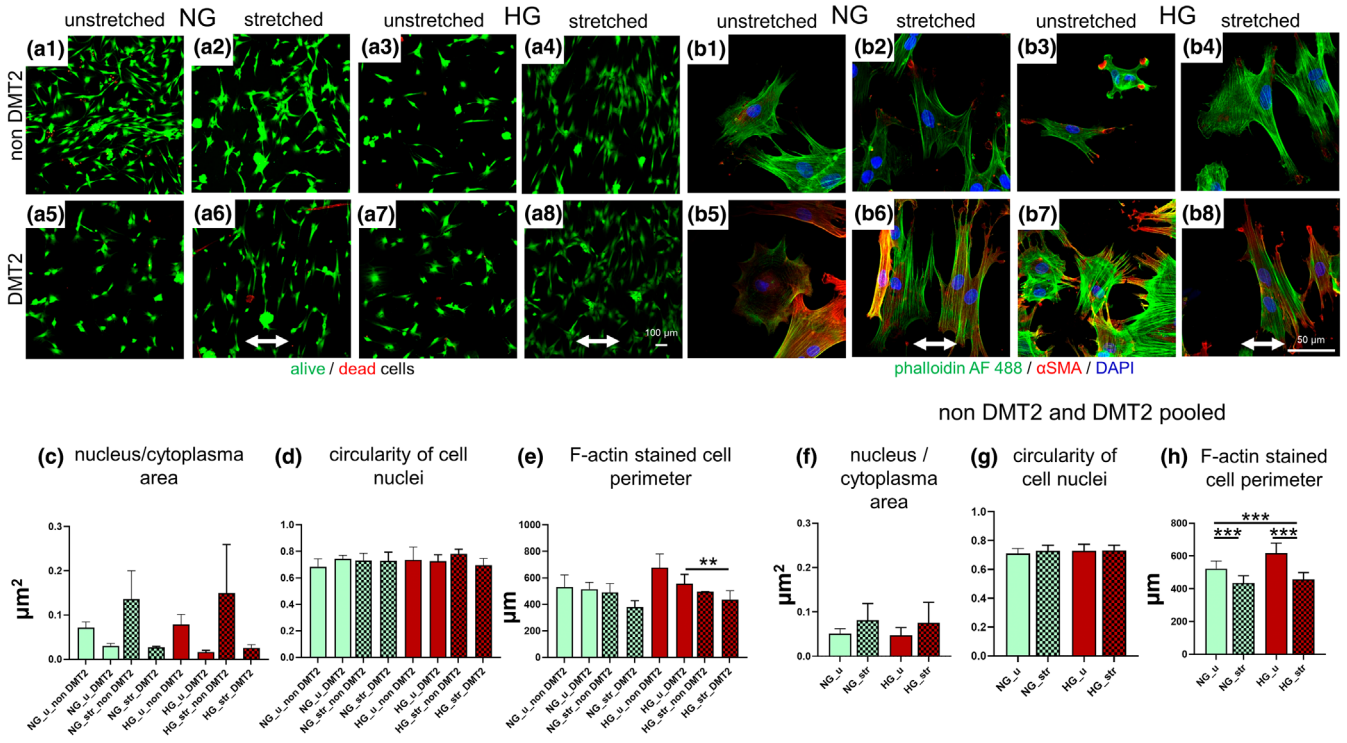

FIGURE 5 Vitality, actin cytoskeletal architecture, shape and size of cell nuclei of tenocytes derived from non diabetic (non DMT2) and diabetic (DMT2) rats exposed to 48 h cyclic stretch or not. In addition cells were exposed to normoglycemic (NG) versus hyperglycemic (HG) conditions. Achilles tendon derived tenocytes were allowed to adhere for 48 h and cyclic stretch (14% at 0.3 Hz) was applied for 48 h with the 6× cell stretcher. Cell vitality after 48 h in unstretched (a1, a3, a5, a7) and stretched (a2, a4, a6, a8) tenocytes under normoglycemic (a1, a2, a5, a6: NG) and hyperglycemic conditions (a3, a4, a7, a8: HG). Green: Vital cells, red: Dead cells. F-actin architecture and alpha smooth muscle actin (αSMA) immunoreactivity depicted by phalloidin-Alexa-Fluor488 stain (green) and αSMA antibodies (red) in unstretched (u) and stretched (str) tenocytes exposed to NG and HG conditions either derived from non DMT2 rats (a1–a4, b1–b4) or DMT2 rats (a5–a8, b5–b8). Cell nuclei were counterstained using 4′,6′-diamidino-2-phenylindole (DAPI). Scale bar: 100 µm (a1–a8), 50 µm (b1–b8). Double-head arrow: Direction of stretch. (c) Ratio of nuclear area (DAPI stain) versus cytoplasma area (F-actin stain), (d) nuclear circularity, (e) F-actin stained cell perimeter of tenocytes. (f–h) Data (f: ratio of the area of cell nuclei, g: nuclear circularity, h: cell perimeter) of cells of non DMT2 and DMT2 rats was pooled. $n = 3$ independent experiments with cells of either non DMT2 or DMT2 rats were conducted. $^{**}p < 0.01$, $^{***}p < 0.005$, paired two-tailed *t*-test.

The nucleus/cytoplasma area increased in response to stretch, but only in cells of non DMT2 animals. It was lower in tenocytes of DMT2 rats (Figure 5c, not significant). Nuclear circularity did not reveal major changes or differences in cells of non T2DM or T2DM rats (Figure 5d).

Unstretched tenocytes (when data of non DMT2 and DMT2 donors were pooled) had generally a significantly larger cell perimeter surrounding the F-actin stained cell area compared to those, stretched for 48 h, both, under NG and HG conditions. Under HG conditions this effect reached also the significance level in tenocytes of exclusively DMT2 rats (Figure 5e).

3.9 | Gene expression of rAS tenocytes in response to cyclic stretch

After stretching, *Hmox1* and *Socs1* expression increased under NG and HG conditions in tenocytes of non DMT2 and diabetic donors compared to the respective NG unstretched controls. For *Hmox1* this effect was significant in tenocytes of DMT2 rats. Pooled data of both donor groups reflected the same significant effect and in addition, a significant increase of *Hmox1* by stretch under HG condition (Figure 6a1–a3).

However, the degree of *Hmox1* induction by stretch under NG was substantially higher in tenocytes from diabetic compared to those of non DMT2 animals (7.12 fold vs. 2.01 fold in mean). For *Socs3*, this stretch induced increase was significant under HG compared to the NG controls in tenocytes of DMT2 rats and when data of both donor groups were pooled.

Nevertheless, HG medium alone, even under unstretched conditions induced the expression of the above mentioned targets in tenocytes of non DMT2 and DMT2 donors compared to NG (Figure 6a–c).

4 | DISCUSSION

The study attempted to address the question whether tenocytes were irreversibly compromised by DMT2 when isolated from DMT2 rats. Hence, these cells might respond to a proinflammatory challenge, HG and stretch in a different manner compared to those isolated from non

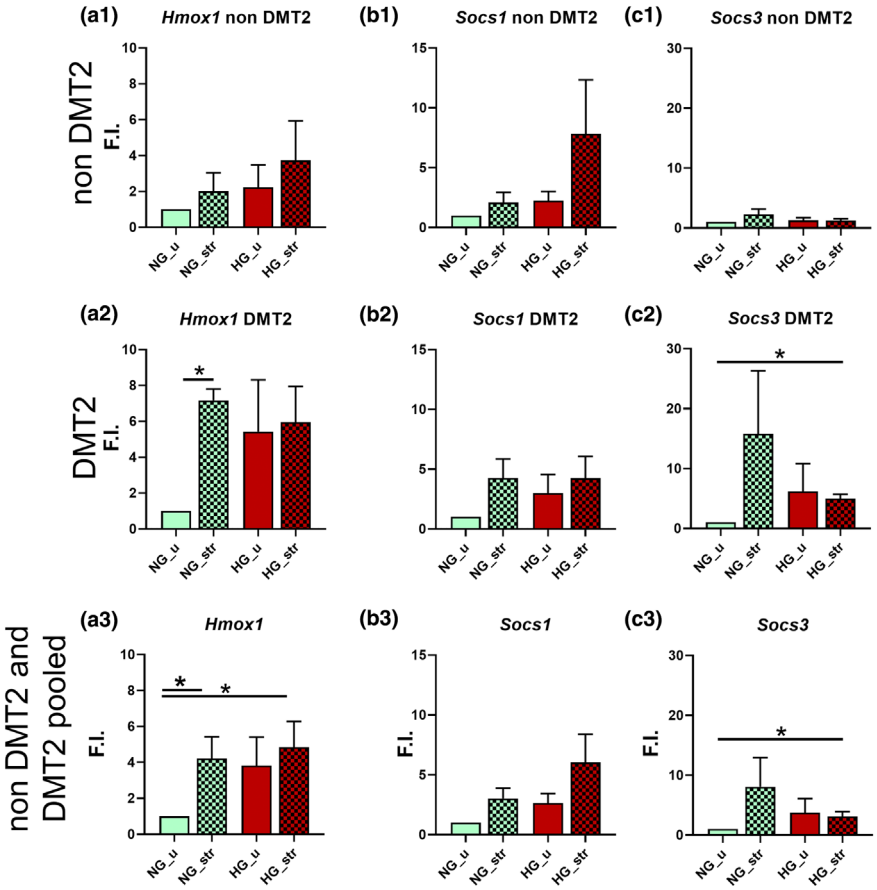

FIGURE 6 Gene expression profile of tenocytes isolated from non diabetic (non DMT2) and diabetic (DMT2) rats in response to cyclic stretching or not for 48 h. In addition, Achilles tendon *derived tenocytes* were exposed to normoglycemic (NG) vs. hyperglycemic (HG) conditions. Tenocytes were allowed to adhere for 48 h and cyclic stretch (14% at 0.3 Hz) was applied for 48 h with the 6× cell stretcher. (a) *Heme oxygenase* (*Hmox1*), (b) *suppressor of cytokine signaling* (*Socs*)*1*, (c) *Socs3* expression after 48 h stretch or remaining unstretched (controls). *Hypoxanthine-guanine-phosphoribosyltransferase (Hprt)1* was used as a reference gene, F.I., fold increase. (a1–c1) Non DMT2, (a2–c2) DMT2, (a3–c3) data of cells of non DMT2 and DMT2 rats was pooled. $n = 3$ independent experiments with tenocytes of either non DMT2 or DMT2 rats. Data was normalized to NG control. $^{*}p < 0.05$, paired two-tailed *t*-test.

DMT2 rats. DMT2 is well known as a risk factor for tendon degeneration and rupture (Vaidya et al., 2023). Hence, differences in tendon histoarchitecture, typical for its degeneration could be expected in tendons of DMT2 rats (Afolabi et al., 2021; Batista et al., 2008; Partridge & Rajbhandari, 2017) and were confirmed in the present study by significantly higher Movin score values in tendons of rats suffering from DMT2. Features such as tendon thickening, collagen disorganization and calcification of the enthesis have been reported in degenerated human AS (Vaidya et al., 2023). The AS midsubstance, formed by the medial and lateral gastrocnemius tendon stands, was investigated in the present study. It showed in diabetic more often compared to the control rats distinct histopathologically detectable signs of degeneration such as a lesser density and alignment of collagen fibers, higher cellularity and more rounded cell nuclei. The summary after evaluation using the Movin score revealed significant differences (Maffulli et al., 2008). This score, was originally approved for human tendons (Maffulli et al., 2004, 2008), but later also used for rAS by other authors (Beytemur et al., 2018; Genc et al., 2018; Lee et al., 2017).

Histopathological alterations of the rAS could be explained by the effects of HG at the molecular level facilitating AGE formation. Highly increased continuous glucose levels could be proven for the donor animals included in this study. Increased amounts of AGEs have been detected in DMT2 tendons (Patel & Carroll, 2023). Characteristics differing between rAS of non DMT2 and DMT2 rats comprised a slightly higher cellularity, a lower collagen type 1 expression and an elevated GAG content as well as αSMA immunoreactivity of tenocytes. Increased αSMA expression was associated with rAS tenocyte migration (Tsai et al., 2008) and implicated in tendon-derived cell contraction (Spector, 2001).

In contrast to the in situ observation in regard to collagen type 1 protein expression, rAS tenocytes of DMT2 rats, cultured for 24 h in NG and HG medium, reflected a slight induction of collagen type 1 synthesis compared to those of non DMT2 rats. This might be explained by the in vitro HG conditions without the highly organized pericellular collagen surrounding the cells in vivo and the effect of continuous hyperinsulinemia, expected in DMT2 in vivo.

In addition, a slight increase in αSMA expression could be observed in cultured rAS tenocytes exposed to TNFα. αSMA was influenced by tenocyte origin either isolated from non DMT2 or DMT2 rats, being higher in tenocytes of DMT2 rats. However, one has to consider that there is generally a high level of αSMA expression in tenocytes or ligamentocytes in two-dimensional monolayer culture (Schwarz et al., 2019) and since monolayers were used in the present study the effect might be covered by 2D mediated αSMA induction. αSMA is implicated in myofibroblast transition during wound healing and scarring (Wang et al., 2008). Overall, the role of αSMA in tendon is not fully explored. It could be associated with stress and tendinopathy (Khan et al., 1999). Nevertheless, vitality of isolated cells was not compromised by DMT2 or HG conditions and remained stably high. The general cell metabolism was also maintained with only a small suppressive trend exerted by TNFα and HG conditions in tenocytes of all donors.

High mRNA levels of *Hmox1*, a gene coding for an antioxidative response enzyme, have been detected in a diabetic rat model which were protective in DMT2 retinopathy (Huo et al., 2022). Accordingly, in the present study *Hmox1* was induced by HG at 4 h, but only in tenocytes from DMT2 rats. In addition, an elevation of *Hmox1* RNA was evoked by TNFα after 24 h, but only in tenocytes from non DMT2 rats underlining the different reaction profile of tenocytes, dependent on their donor history. The induction of this enzyme by TNFα was also previously demonstrated in endothelial cells (Terry et al., 1999).

SOCS1 and SOCS3 play a substantial role in negative feedback regulation of proinflammatory cytokines in tenocytes. Both genes were significantly induced by TNFα in human Hamstring tendon derived tenocytes of healthy donors after 24 h in a previous study (John et al., 2010). Interestingly, at the same time point (24 h) no major trend induced by TNFα could be shown in the present study. Possibly, an earlier time point of analysis not included in the present study might show this induction also in the rAS tenocyte model. Nevertheless, HG led to a twofold induction of *Socs1* and *Socs3* at 4 h in tenocytes from DMT2 animals.

Differences in the gene expression of *Socs1* compared with *Socs3* might be influenced by the fact that the cytokine suppressors activate a different set of transcription factors, the signal transducers and activators of transcription (STAT)1 (by SOCS1) vs. STAT3 (by SOCS3) to trigger the Janus kinase (JAK)/STAT signaling pathway (de Souza et al., 2011).

Appropriate exercise is a therapeutic strategy to improve tendon healing (Eliasson et al., 2012a, 2012b). Hence, a moderate uniaxial cyclic stretch training was applied in this study (0.3 Hz, 14%, 48 h) based on the promising effects revealed by a previous study with cruciate ligamentocytes (Gögele et al., 2021). It has been shown that exercise could increase peritendinous IL-6 levels in rAS in vivo (Katsma et al., 2017). In another study cyclic strain (24 h, 1 Hz, 8%) induced vascular endothelial growth factor (VEGF) and hypoxia inducible factor (HIFα), whereas a lower frequency (0.5 Hz) inhibited VEGF expression in cultured rAS tenocytes (Petersen et al., 2004). Gao et al., studied different training protocols for rAS stem cells and found an early induction of c-fos mRNA, suggesting that stem cell differentiation is influenced at an early stage by stretch (Gao et al., 2017). In the present study in accordance with previous observations (Gögele et al., 2021; Raimondi et al., 2018) tenocytes responded in a typical manner to cyclic stretch with cell alignment to zero stretch direction with a maintained high rate of cell viability, irrespectively of donor and NG or HG conditions.

F-actin fibers are crossing through the cells ending in focal adhesion sites. Focal adhesion kinase, associated with focal adhesions, is known to be activated by cyclic stretch mediating Ca++ influx into the tenocytes (Huang et al., 2022). However, the number of focal adhesions was not counted in the present study. The F-actin stain showed fiber alignment. It was used to determine the cytoplasmic area and to get a relation to the size of the cell nuclei by DAPI stain.

Tenocytes derived from DMT2 donors had a substantial smaller nucleus/cytoplasma ratio than those from non DMT2 rats. This seems, on the first view to be in contrast to a previous study analyzing the ratio between both, cytoplasma and nucleus, in extrafoliated buccal mucosa cells of non DMT2 and DMT2 patients (Sahay et al., 2017). This ratio and its regulation might be cell-type specific. Features of nuclear degeneration were described by the authors in the cited study. Nevertheless, the present study showed no increase in cell death or morphological indicators of nuclear degeneration.

Under stretch, the area of the cell nucleus to cytoplasm ratio decreased only slightly and only in cells of non DMT2 donors. The nuclear area might be influenced by cell cyclus stage. A higher proliferation rate can also be associated with smaller cell perimeter since after cell division, the daughter cells need time to grow to their regular size. A higher rate of cell division might mask the effects of stretching described before (Gögele et al., 2021). Cell nucleus size might also be a feature of differing gene activity and chromatin condensation as well as alterations of the cell nuclear lamina architecture by lamin structure (Dahl et al., 2008). Interestingly the cell perimeter was significantly smaller in tenocytes exposed to cyclic stretch, both under NG and HG conditions. It remains unclear whether stretched tenocytes were more convex and hence, cell volume could be similar.

Stretching had pronounced effects on gene expression of regulatory mediators: the antioxidative enzyme gene *Hmox1* was significantly induced by cyclic stretch in tenocytes, particularly in those of DMT2 donors. Despite no data are available for tenocytes in agreement with this present observation, it has been reported that *Hmox1* was slightly induced in synovial fibroblasts by cyclic stretch (Takao et al., 2011).

Socs3 gene activity was induced by cyclic stretching, however, the significance level was only achieved under HG conditions in cells of both donor types or those of DMT2 rats. Based on the fact that literature related to the regulation of these transcription factors by mechanical stress in tendons was not available, one could hypothesize that mechanical stress induces these negative feedback regulators of proinflammatory cytokine signaling.

5 | CONCLUSIONS

A significant in situ AS degeneration could be found in AS of DMT2 rats. Tenocytes isolated from non DMT2 and DMT2 rAS showed

differences in their response to the glucose microenvironment and stretching e.g., in regard to *Hmox1* regulation. The significant induction of cytoprotective *Hmox1* by stretching was very high in cells of DMT2 rats under NG conditions and apparently overlapped with an inductive effect of HG under HG conditions. The negative cytokine regulator *Socs3* was significantly upregulated under HG conditions.

Taken together, the reaction profile of tenocytes isolated from DMT2 and non DMT2 rat groups slightly differed with an enhanced stress response in cells of DMT2 donors. This has to be considered in healing of DMT2 tendons and in searching for future tissue engineering strategies applied to support healing of injured AS of DMT2 patients.

AUTHOR CONTRIBUTIONS

Conceptualization: G.S.-T., B.H. Methodology: N.F., S.H., C.G., E.F., J.K., M.K. Validation: N.F., S.H., C.G., E.F. Investigation: N.F., S.H., C.G., C.W., E.F., G.S.-T., M.K. Resources: B.H., J.K., G.S.-T. M.K. Data curation: N.F., S.H., C.G., G.S.-T. Writing—original draft preparation: G.S.-T. Writing—review and editing: N.F., S.H., G.S.-T., N.F., S.H. Visualization: G.S.-T., C.G., N.F., S.H., E.F. Supervision: G.S.-T., C.G. Project administration: G.S.-T. Funding acquisition: G.S.-T.

ACKNOWLEDGEMENTS

The authors thank Benjamin Kohl for support. The study (RUF 55.2.2-2532-2-729-17) providing the rats from which the tendons and tenocytes were isolated post mortem was supported by the Kerscher'sche Diabetes Research Foundation (grant numbers SZ_FP_008.18 and SZ_FP_164.20) and DFG Schu1979/14-1. Funding sources had no involvement in study design, collection, analysis and interpretation of data, writing of the report and decision to submit the article for publication.

DATA AVAILABILITY STATEMENT

Data available on request from the authors.

ORCID

Clemens Gögele https://orcid.org/0000-0002-7086-9743
Gundula Schulze-Tanzil https://orcid.org/0000-0002-9807-9532

REFERENCES

Afolabi, B.I., Idowu, B.M. & Onigbinde, S.O. (2021) Achilles tendon degeneration on ultrasound in type 2 diabetic patients. *Journal of Ultrasonography*, 20, e291–e299.

Aicale, R., Oliviero, A. & Maffulli, N. (2020) Management of Achilles and patellar tendinopathy: what we know, what we can do. *Journal of Foot and Ankle Research*, 13, 59.

Attia, R.A., Fattah, S.A. & Nasralla, M.M. (2021) Concomitant administration of sitagliptin and rutin improves the adverse hepatic alterations in streptozotocin-induced diabetes mellitus in albino rats: an overview of the role of alpha smooth muscle actin. *Folia Morphologica*, 80, 870–880.

Ballal, M.S., Walker, C.R. & Molloy, A.P. (2014) The anatomical footprint of the Achilles tendon: a cadaveric study. *The Bone & Joint Journal*, 96, 1344–1348.

Batista, F., Nery, C., Pinzur, M., Monteiro, A.C., de Souza, E.F., Felippe, F.H. et al. (2008) Achilles tendinopathy in diabetes mellitus. *Foot & Ankle International*, 29, 498–501.

Beytemur, O., Yuksel, S., Tetikkurt, U.S., Genc, E., Olcay, E. & Gulec, A. (2018) Isotretinoin induced achilles tendinopathy: histopathological and biomechanical evaluation on rats. *Acta Orthopaedica et Traumatologica Turcica*, 52, 387–391.

Bezerra, M.A., da Silva Nery, C., De Castro Silveira, P.V., De Mesquita, G.N., De Gomes Figueiredo, T., Teixeira, M.F. et al. (2016) Previous physical exercise slows down the complications from experimental diabetes in the calcaneal tendon. *Muscles, Ligaments and Tendons Journal*, 6, 97–103.

Cannata, F., Vadala, G., Ambrosio, L., Napoli, N., Papalia, R., Denaro, V. et al. (2021) The impact of type 2 diabetes on the development of tendinopathy. *Diabetes/Metabolism Research and Reviews*, 37, e3417.

Chbinou, N. & Frenette, J. (2004) Insulin-dependent diabetes impairs the inflammatory response and delays angiogenesis following Achilles tendon injury. *American Journal of Physiology. Regulatory, Integrative and Comparative Physiology*, 286, R952–R957.

Cherng, S., Young, J. & Ma, H. (2008) Alpha-smooth muscle actin (α-SMA). *The Journal of American Science*, 4, 7–9.

Dahl, K.N., Ribeiro, A.J. & Lammerding, J. (2008) Nuclear shape, mechanics, and mechanotransduction. *Circulation Research*, 102, 1307–1318.

de Oliveira, R.R., Bezerra, M.A., De Lira, K.D., Novaes, K.A., Teixeira, M.F., Chaves Cde, C. et al. (2012) Aerobic physical training restores biomechanical properties of Achilles tendon in rats chemically induced to diabetes mellitus. *Journal of Diabetes and its Complications*, 26, 163–168.

de Oliveira, R.R., De Lira, K.D., Silveira, P.V., Coutinho, M.P., Medeiros, M.N., Teixeira, M.F. et al. (2011) Mechanical properties of achilles tendon in rats induced to experimental diabetes. *Annals of Biomedical Engineering*, 39, 1528–1534.

de Souza, J.A., Nogueira, A.V., de Souza, P.P., Cirelli, J.A., Garlet, G.P., Rossa, C. Jr. (2011) Expression of suppressor of cytokine signaling 1 and 3 in ligature-induced periodontitis in rats. *Archives of Oral Biology*, 56(10), 1120–1128.

Egemen, O., Ozkaya, O., Ozturk, M.B., Sen, E., Akan, M., Sakiz, D. et al. (2012) The biomechanical and histological effects of diabetes on tendon healing: experimental study in rats. *Journal of Hand and Microsurgery*, 4, 60–64.

Egerbacher, M., Arnoczky, S.P., Caballero, O., Lavagnino, M. & Gardner, K.L. (2008) Loss of homeostatic tension induces apoptosis in tendon cells: an in vitro study. *Clinical Orthopaedics and Related Research*, 466, 1562–1568.

El-Huneidi, W., Anjum, S., Bajbouj, K., Abu-Gharbieh, E. & Taneera, J. (2021) The coffee Diterpene, Kahweol, ameliorates pancreatic beta-cell function in streptozotocin (STZ)-treated rat INS-1 cells through NF-kB and p-AKT/Bcl-2 pathways. *Molecules*, 26(17), 5167.

Eliasson, P., Andersson, T. & Aspenberg, P. (2012a) Achilles tendon healing in rats is improved by intermittent mechanical loading during the inflammatory phase. *Journal of Orthopaedic Research*, 30, 274–279.

Eliasson, P., Andersson, T. & Aspenberg, P. (2012b) Influence of a single loading episode on gene expression in healing rat Achilles tendons. *Journal of Applied Physiology*, 1985(112), 279–288.

Fernandez, P., Guillen, M.I., Gomar, F. & Alcaraz, M.J. (2003) Expression of heme oxygenase-1 and regulation by cytokines in human osteoarthritic chondrocytes. *Biochemical Pharmacology*, 66, 2049–2052.

Gao, S., Tang, K., Zhang, J., Yang, Z., Cui, H., Li, P. et al. (2017) Effect of cyclic stretch on expression of c-fos gene in rat Achilles-derived tendon stem cells. *Zhongguo Xiu Fu Chong Jian Wai Ke Za Zhi*, 31, 85–90.

Gardner, K., Lavagnino, M., Egerbacher, M. & Arnoczky, S.P. (2012) Re-establishment of cytoskeletal tensional homeostasis in lax tendons occurs through an actin-mediated cellular contraction of the extracellular matrix. *Journal of Orthopaedic Research*, 30, 1695–1701.

Genc, E., Beytemur, O., Yuksel, S., Eren, Y., Caglar, A., Kucukyildirim, B.O. et al. (2018) Investigation of the biomechanical and

histopathological effects of autologous conditioned serum on healing of Achilles tendon. *Acta Orthopaedica et Traumatologica Turcica*, 52, 226–231.

Gögele, C., Hoffmann, C., Konrad, J., Merkel, R., Schwarz, S., Tohidnezhad, M. et al. (2021) Cyclically stretched ACL fibroblasts emigrating from spheroids adapt their cytoskeleton and ligament-related expression profile. *Cell and Tissue Research*, 384, 675–690.

Guillen, M., Megias, J., Gomar, F. & Alcaraz, M. (2008) Haem oxygenase-1 regulates catabolic and anabolic processes in osteoarthritic chondrocytes. *The Journal of Pathology*, 214, 515–522.

Guney, A., Vatansever, F., Karaman, I., Kafadar, I.H., Oner, M. & Turk, C.Y. (2015) Biomechanical properties of Achilles tendon in diabetic vs. non-diabetic patients. *Experimental and Clinical Endocrinology & Diabetes*, 123, 428–432.

Hess, G.W. (2010) Achilles tendon rupture: a review of etiology, population, anatomy, risk factors, and injury prevention. *Foot & Ankle Specialist*, 3, 29–32.

Huang, Y.T., Wu, Y.F., Wang, H.K., Yao, C.J., Chiu, Y.H., Sun, J.S. et al. (2022) Cyclic mechanical stretch regulates the AMPK/Egr1 pathway in tenocytes via Ca^{2+}-mediated mechanosensing. *Connective Tissue Research*, 63, 590–602.

Huo, J., Meng, G. & Jiang, X. (2022) Influence of heme oxygenase-1 on rats with diabetic retinopathy through ERK1/2 signaling pathway. *Cellular and Molecular Biology (Noisy-le-Grand, France)*, 68, 92–97.

Immenschuh, S. & Ramadori, G. (2000) Gene regulation of heme oxygenase-1 as a therapeutic target. *Biochemical Pharmacology*, 60, 1121–1128.

John, T., Lodka, D., Kohl, B., Ertel, W., Jammrath, J., Conrad, C. et al. (2010) Effect of pro-inflammatory and immunoregulatory cytokines on human tenocytes. *Journal of Orthopaedic Research*, 28, 1071–1077.

Katsma, M.S., Patel, S.H., Eldon, E., Corbell, K.A., Shimkus, K.L., Fluckey, J.D. et al. (2017) The influence of chronic IL-6 exposure, in vivo, on rat Achilles tendon extracellular matrix. *Cytokine*, 93, 10–14.

Khan, K.M., Cook, J.L., Bonar, F., Harcourt, P. & Astrom, M. (1999) Histopathology of common tendinopathies. Update and implications for clinical management. *Sports Medicine*, 27, 393–408.

Kim, D.H., Noh, S.U., Chae, S.W., Kim, S.J. & Lee, Y.T. (2021) Altered differentiation of tendon-derived stem cells in diabetic conditions mediated by macrophage migration inhibitory factor. *International Journal of Molecular Sciences*, 22, 8983.

Kim, Y.M., Jeon, E.S., Kim, M.R., Lee, J.S. & Kim, J.H. (2008) Bradykinin-induced expression of alpha-smooth muscle actin in human mesenchymal stem cells. *Cellular Signalling*, 20, 1882–1889.

Korntner, S., Kunkel, N., Lehner, C., Gehwolf, R., Wagner, A., Augat, P. et al. (2017) A high-glucose diet affects Achilles tendon healing in rats. *Scientific Reports*, 7, 780.

Lattouf, R., Younes, R., Lutomski, D., Naaman, N., Godeau, G., Senni, K. et al. (2014) Picrosirius red staining: a useful tool to appraise collagen networks in normal and pathological tissues. *The Journal of Histochemistry and Cytochemistry*, 62, 751–758.

Lee, J.M. & Veres, S.P. (2019) Advanced glycation end-product cross-linking inhibits biomechanical plasticity and characteristic failure morphology of native tendon. *Journal of Applied Physiology*, 1985(126), 832–841.

Lee, S.Y., Chieh, H.F., Lin, C.J., Jou, I.M., Sun, Y.N., Kuo, L.C. et al. (2017) Characteristics of sonography in a rat Achilles tendinopathy model: possible non-invasive predictors of biomechanics. *Scientific Reports*, 7, 5100.

Li, Y., Fessel, G., Georgiadis, M. & Snedeker, J.G. (2013) Advanced glycation end-products diminish tendon collagen fiber sliding. *Matrix Biology*, 32, 169–177.

Lui, P.P.Y. (2017) Tendinopathy in diabetes mellitus patients-epidemiology, pathogenesis, and management. *Scandinavian Journal of Medicine & Science in Sports*, 27, 776–787.

Maffulli, N., Longo, U.G., Franceschi, F., Rabitti, C. & Denaro, V. (2008) Movin and Bonar scores assess the same characteristics of tendon histology. *Clinical Orthopaedics and Related Research*, 466, 1605–1611.

Maffulli, N., Testa, V., Capasso, G., Ewen, S.W., Sullo, A., Benazzo, F. et al. (2004) Similar histopathological picture in males with Achilles and patellar tendinopathy. *Medicine and Science in Sports and Exercise*, 36, 1470–1475.

Partridge, L. & Rajbhandari, S. (2017) Achilles tendon in diabetes. *Current Diabetes Reviews*, 13, 424–427.

Patel, S.H. & Carroll, C.C. (2023) Impact of elevated serum advanced glycation end products and exercise on intact and injured murine tendons. *Connective Tissue Research*, 64, 161–174.

Patel, S.H., Yue, F., Saw, S.K., Foguth, R., Cannon, J.R., Shannahan, J.H. et al. (2019) Advanced glycation end-products suppress mitochondrial function and proliferative capacity of Achilles tendon-derived fibroblasts. *Scientific Reports*, 9, 12614.

Petersen, W., Varoga, D., Zantop, T., Hassenpflug, J., Mentlein, R. & Pufe, T. (2004) Cyclic strain influences the expression of the vascular endothelial growth factor (VEGF) and the hypoxia inducible factor 1 alpha (HIF-1alpha) in tendon fibroblasts. *Journal of Orthopaedic Research*, 22, 847–853.

Poulsen, R.C., Knowles, H.J., Carr, A.J. & Hulley, P.A. (2014) Cell differentiation versus cell death: extracellular glucose is a key determinant of cell fate following oxidative stress exposure. *Cell Death & Disease*, 5, e1074.

Raimondi, M.T., Lagana, M., Conci, C., Crestani, M., Di Giancamillo, A., Gervaso, F. et al. (2018) Development and biological validation of a cyclic stretch culture system for the ex vivo engineering of tendons. *The International Journal of Artificial Organs*, 41, 400–412.

Sahay, K., Rehani, S., Kardam, P., Kumra, M., Sharma, R. & Singh, N. (2017) Cytomorphometric analysis and morphological assessment of oral exfoliated cells in type 2 diabetes mellitus and healthy individuals: a comparative study. *Journal of Cytology*, 34, 27–33.

Schefe, J.H., Lehmann, K.E., Buschmann, I.R., Unger, T. & Funke-Kaiser, H. (2006) Quantitative real-time RT-PCR data analysis: current concepts and the novel "gene expression's CT difference" formula. *Journal of Molecular Medicine*, 84, 901–910.

Schulze-Tanzil, G.G., Delgado-Calcares, M., Stange, R., Wildemann, B. & Docheva, D. (2022) Tendon healing: a concise review on cellular and molecular mechanisms with a particular focus on the Achilles tendon. *Bone & Joint Research*, 11, 561–574.

Schwarz, S., Gögele, C., Ondruschka, B., Hammer, N., Kohl, B. & Schulze-Tanzil, G. (2019) Migrating myofibroblastic iliotibial band-derived fibroblasts represent a promising cell source for ligament reconstruction. *International Journal of Molecular Sciences*, 20, 1972.

Shi, L., Li, Y.J., Dai, G.C., Lin, Y.C., Li, G., Wang, C. et al. (2019) Impaired function of tendon-derived stem cells in experimental diabetes mellitus rat tendons: implications for cellular mechanism of diabetic tendon disorder. *Stem Cell Research & Therapy*, 10, 27.

Shi, L., Lu, P.P., Dai, G.C., Li, Y.J. & Rui, Y.F. (2021) Advanced glycation end productions and tendon stem/progenitor cells in pathogenesis of diabetic tendinopathy. *World Journal of Stem Cells*, 13, 1338–1348.

Skutek, M., van Griensven, M., Zeichen, J., Brauer, N. & Bosch, U. (2001) Cyclic mechanical stretching enhances secretion of interleukin 6 in human tendon fibroblasts. *Knee Surgery, Sports Traumatology, Arthroscopy*, 9, 322–326.

Spector, M. (2001) Musculoskeletal connective tissue cells with muscle: expression of muscle actin in and contraction of fibroblasts, chondrocytes, and osteoblasts. *Wound Repair and Regeneration*, 9, 11–18.

Takao, M., Okinaga, T., Ariyoshi, W., Iwanaga, K., Nakamichi, I., Yoshioka, I. et al. (2011) Role of heme oxygenase-1 in inflammatory response induced by mechanical stretch in synovial cells. *Inflammation Research*, 60, 861–867.

Tarantino, D., Mottola, R., Resta, G., Gnasso, R., Palermi, S., Corrado, B. et al. (2023) Achilles tendinopathy pathogenesis and management:

A narrative review. *International Journal of Environmental Research and Public Health*, 20, 6681.

Terry, C.M., Clikeman, J.A., Hoidal, J.R. & Callahan, K.S. (1999) TNF-alpha and IL-1alpha induce heme oxygenase-1 via protein kinase C, Ca^{2+}, and phospholipase A2 in endothelial cells. *The American Journal of Physiology*, 276, H1493–H1501.

Tognoloni, A., Bartolini, D., Pepe, M., Di Meo, A., Porcellato, I., Guidoni, K. et al. (2023) Platelets rich plasma increases antioxidant Defenses of tenocytes via Nrf2 signal pathway. *International Journal of Molecular Sciences*, 24, 13299.

Tsai, W.C., Chen, J.Y., Pang, J.H., Hsu, C.C., Lin, M.S. & Chieh, L.W. (2008) Therapeutic ultrasound stimulation of tendon cell migration. *Connective Tissue Research*, 49, 367–373.

Vaidya, R., Lake, S.P. & Zellers, J.A. (2023) Effect of diabetes on tendon structure and function: not limited to collagen crosslinking. *Journal of Diabetes Science and Technology*, 17, 89–98.

Wang, J., Dodd, C., Shankowsky, H.A., Scott, P.G., Tredget, E.E. & Wound Healing Research Group. (2008) Deep dermal fibroblasts contribute to hypertrophic scarring. *Laboratory Investigation*, 88, 1278–1290.

Yuan, Z., Zhu, X., Dai, Y., Shi, L., Feng, Z., Li, Z. et al. (2024) Analysis of differentially expressed genes in torn rotator cuff tendon tissues in diabetic patients through RNA-sequencing. *BMC Musculoskeletal Disorders*, 25, 31.

Zhang, T., Tian, J., Fan, J., Liu, X. & Wang, R. (2023) Exercise training-attenuated insulin resistance and liver injury in elderly pre-diabetic patients correlates with NLRP3 inflammasome. *Frontiers in Immunology*, 14, 1082050.

SUPPORTING INFORMATION

Additional supporting information can be found online in the Supporting Information section at the end of this article.

How to cite this article: Fleischmann, N., Hofmann, S., Gögele, C., Frank, E., Werner, C., Kokozidou, M. et al. (2026) Achilles tenocytes from diabetic and non diabetic donors exposed to hyperglycemia respond differentially to inflammatory stimuli and stretch. *Journal of Anatomy*, 248, 675–688. Available from: https://doi.org/10.1111/joa.14207